Published in final edited form as:
Neuropharmacology. 2014 September ; 84: 1–12. doi:10.1016/j.neuropharm.2014.04.011.

Necessary, but not Sufficient: Insights into the Mechanisms of mGluR Mediated Long Term Depression from a Rat Model of Early Life Seizures

Paul B. Bernard[1], **Anna M. Castano**[1], **K. Ulrich Bayer**[2,4], and **Tim. A. Benke**[1,2,3,4,5]

[1]Department of Pediatrics, University of Colorado, School of Medicine

[2]Department of Neuroscience Graduate Program, University of Colorado, School of Medicine

[3]Department of Neurology, University of Colorado, School of Medicine

[4]Department of Pharmacology, University of Colorado, School of Medicine

[5]Department of Otolaryngology, University of Colorado, School of Medicine

Abstract

Using the rat model of early life seizures (ELS), which has exaggerated mGluR mediated long-term depression of synaptic strength (mGluR-LTD) in adulthood, we probed the signaling cascades underlying mGluR-LTD induction. Several inhibitors completely blocked mGluR-LTD in control but not in ELS rats: the proteasome, the mammalian target of rapamycin (mTOR), S6 kinase (S6K), or L-type voltage-gated calcium channels (L-type VGCC). Inhibition of the Ca^{2+}/calmodulin-dependent protein kinase II (CaMKII) resulted in a near complete block of mGluR-LTD in control rats and a slight reduction of mGluR-LTD in ELS rats. “Autonomous” CaMKII was found to be upregulated in ELS rats, while elevated S6K activity, which is stimulated by mTOR, was described previously. Thus, modulation of each of these factors was necessary for mGluR-LTD induction in control rats, but even their combined, permanent activation in the ELS rats was not sufficient to individually support mGluR-LTD induction following ELS. This implies that while these factors may act sequentially in controls to mediate mGluR-LTD, this is no longer the case after ELS. In contrast, activated ERK was found to be significantly down-regulated in ELS rats. Inhibition of MEK/ERK activation in control rats elevated mGluR-LTD to the exaggerated levels seen in ELS rats. Together, these results elucidate both the mechanisms that persistently enhance mGluR-LTD after ELS and the mechanisms underlying normal mGluR-LTD by providing evidence for multiple, convergent pathways that mediate mGluR-LTD induction.

Corresponding author: Tim A. Benke, University of Colorado Denver, School of Medicine, 12800 E 19th, MS8102, Denver, CO 80045, tim.benke@ucdenver.edu; 303 724-3568; 303 724 2439.

Author responsibilities

PBB, AMC and TAB designed, performed and analyzed the experiments. KUB helped in experimental design and provided reagents. PBB and TAB co-wrote the paper, all proof-read the paper; TAB supervised the project. The authors declare no conflicts of interest.

With our prior work, this ties these signaling cascades to the ELS behavioral phenotype that includes abnormal working memory, fear conditioning and socialization.

Keywords

Early Life Seizure; Long-term depression; Metabotropic glutamate receptor; CaMKII; Voltage gated calcium channels; Autism

Introduction

The mechanisms underlying the induction of metabotropic glutamate receptor (mGluR) (Conn and Pin, 1997;Nakanishi, 1994;Pin and Duvoisin, 1995) mediated long term depression (mGluR-LTD) are not yet fully and clearly defined (Malenka and Bear, 2004; Luscher and Huber, 2010; Gladding et al., 2009). While studying an early life seizure (ELS) rat model that does not result in later epilepsy, we have previously reported an increase in mGluR-LTD several months following a single episode of ELS in the rat in the absence of changes in basal neural transmission and neuronal morphology (Bernard et al., 2013; Cornejo et al., 2007). In adult rodents, long-term depression is primarily induced through activation of mGluRs that results in protein translation (Gladding et al., 2009; Luscher and Huber, 2010). Synaptically localized (Stefani et al., 2004) and phosphorylated Fragile X Mental Retardation Protein (FMRP) acts as a negative regulator of translation under basal conditions (Narayanan et al., 2007; Bassell and Warren, 2008), thus regulating and limiting the amount of mGluR-LTD. In current schema, mGluR-mediated signaling first leads to activation of protein phosphatase 2A (PP2A) and dephosphorylation of FMRP (thereby activating translation) while further mGluR-mediated stimulation activates the mammalian target of rapamycin (mTOR) pathway, secondarily leading to re-phosphorylation of FMRP via p70-S6 kinase (S6K), stalling translation and limiting the magnitude of mGluR-LTD (Ceman et al., 2003; Narayanan et al., 2007; Bassell and Warren, 2008; Narayanan et al., 2008). Following mGluR activation, a fraction of FMRP is ubiquitinated and subsequently degraded by the proteasome (Hou et al., 2006). Blocking proteasome mediated degradation and/or ubiquitination prevents the induction of mGluR-LTD in wild type mice, but not in FMRP knockouts (Hou et al., 2006) (but see (Citri et al., 2009)). mTOR, a central regulator of cell growth, proliferation, autophagy, and translation (Hay and Sonenberg, 2004; Klann and Dever, 2004; Sarbassov et al., 2005), is thought to exert pre-eminent influence on mGluR-LTD via its control over local protein synthesis (Tang et al., 2002). The changes to adult mGluR-LTD following ELS were, in part, related to alterations in the FMRP, PP2A, S6K (FMRP/PP2A/S6K) signaling complex that regulates local protein synthesis and subsequently mGluR-LTD. mGluR-LTD induction remains critically dependent and convergent on protein synthesis (Huber et al., 2000) in this model (Bernard et al., 2013). However many other proteins are believed to function in concert with FMRP/S6K/PP2A to exert control over mGluR-LTD. Herein we further explore the roles of other proteins in mGluR-LTD and investigate whether or not they are altered following ELS.

Traditionally Ca^{2+}/calmodulin-dependent protein kinase II (CaMKII) has been regarded as a crucial mediator of long term potentiation (Malenka and Bear, 2004; Coultrap and Bayer,

2012; Lisman et al., 2012). Through the use of relatively non-selective antagonists (Coultrap et al., 2011), recent evidence suggests that CaMKII may contribute to the induction of mGluR-LTD (Mockett et al., 2011). The specific mechanisms by which CaMKII exerts its control over mGluR-LTD and associated protein synthesis are still unknown. The involvement of CaMKII in mGluR-LTD implicates the involvement of a calcium source associated with mGluR activation but this source has not yet been identified (Mockett et al., 2011).

The role of mitogen-activated protein kinase/extracellular signal-regulated kinase 1/2 (MEK/ERK1/2) signaling is complicated and unclear in mediating the induction of mGluR-LTD. MEK/ERK1/2 is involved in mGluR associated protein synthesis (Osterweil et al., 2010; Mockett et al., 2011). Activation of mGluRs results in the phosphorylation of ERK and blocking ERK is reported to block mGluR-LTD (Banko et al., 2006; Gallagher et al., 2004). In contrast to these findings, a Tuberous sclerosis complex (TSC) rodent model displays elevated levels of ERK activation which correlates with reduced mGluR-LTD. Loss of mGluR-LTD in this TSC model can be rescued using U0126, an inhibitor of ERK signaling (Chevere-Torres et al., 2012), strongly suggesting that elevated ERK signaling is responsible for the reduced mGluR-LTD in this TSC model.

Using biochemistry and electrophysiology in rat hippocampal CA1 slices from ELS and control rats, we found evidence for multiple, convergent pathways that mediate mGluR-LTD induction. While modulation of these pathways inhibited mGluR-LTD induction in control rats, this was not necessarily the case following ELS. This is consistent with biochemistry and demonstrates that mTOR, S6K, proteasome, voltage-gated calcium channels and CaMKII are each necessary but not sufficient for the induction of mGluR-LTD. MEK/ERK1/2 signaling regulated the amount of mGluR-LTD induced that was consistent with reduced ERK phosphorylation and the notion that ERK phosphorylation may regulate the “set-point” for the magnitude of mGluR-LTD. As a whole, these results indicate that several signaling processes must be activated simultaneously in order for the successful induction of mGluR-LTD. In ELS rats, due to permanently altered (enhanced) signaling pathways, several of these steps are perpetually “in place”, resulting in exaggerated mGluR-LTD even in the presence of inhibitors that would normally prevent the induction of mGluR-LTD.

Materials and Methods

Animals

All studies conformed to the requirements of the National Institutes of Health *Guide for the Care and Use of Laboratory Rats* and were approved by the Institutional Animal Care and Use subcommittee of the University of Colorado Health Sciences Center. Timed-pregnant Sprague Dawley rats (Charles Rivers Labs, Wilmington, MA) gave birth in-house. All rodents were housed in micro-isolator cages with water and chow available *ad libitum*.

Seizure Induction

Kainic acid (KA), a fixed glutamate analog (Dingledine et al., 1999), was used to induce temporal-lobe seizures (Tremblay et al., 1984) as done in previous studies (Bernard et al.,

2013; Cornejo et al., 2007; Cornejo et al., 2008). Male rat pups were subcutaneously injected with KA (2 mg/kg; Tocris, Ellisville, MO) on P7 (P0 defined as the date of birth) resulting in discontinuous behavioral and electrical seizure activity lasting up to three hours (Dzhala et al., 2005). Mortality was less than 3%. Onset of seizure activity occurred within 30 min of injection and was characterized by intermittent myoclonic jerks, generalized tonic-clonic jerks, scratching, “swimming”, and “wet-dog shakes.” Control male rat pups were injected with an equivalent volume of 0.9% saline. Male pups were chosen in order to eliminate the effects of hormonal cycles on behavior. Rats were then tagged with a microchip (Avid Identification Systems, Norco, CA) so that experimenters remained blinded to the treatment. Offspring were returned to their dam after observable seizure activity ceased. Rats were weaned and separated according to gender at P20–22. At P60–90, electrophysiological and biochemical analyses were undertaken with male rats.

Hippocampal Slice Preparation and Electrophysiology

As done previously(Bernard et al., 2013;Cornejo et al., 2007), following rapid decapitation and removal of the brain, sagittal hippocampal slices (400 μm) were made using a vibratome (Leica VT 1200, Buffalo Grove, IL) in ice-cold sucrose artificial cerebral spinal fluid (sACSF: 206 mM sucrose, 2.8 mM KCl, 1 mM $CaCl_2$, 3 mM $MgSO_4$, 1.25 mM NaH_2PO_4, 26 mM $NaHCO_3$, 10 mM D-glucose and bubbled with 95%/5% O_2/CO_2) (Kuenzi et al., 2000). Following removal of CA3, slices were recovered in a submersion type chamber perfused with oxygenated artificial cerebral spinal fluid (ACSF: 124 mM NaCl, 3 mM KCl, 1 mM $MgSO_4$, 2 mM $CaCl_2$, 1.2 mM NaH_2PO_4, 26 mM NaHCO3, 10 mM D-glucose and bubbled with 95%/5% O_2/CO_2) at 28°C for at least 90 min and then submerged in a recording chamber perfused with ACSF. All electrophysiology was performed in the CA1 region at 28°C. Two twisted-tungsten bipolar stimu lating electrodes were offset in the CA1 to stimulate two independent Schaffer collateral-commissural pathways using a constant current source (WPI, Sarasota, FL) with a fixed duration (20 μs), each at a rate of 0.033 Hz. Field excitatory post-synaptic potentials (fEPSPs) were recorded from the stratum radiatum region of CA1 using a borosilicate glass (WPI, Sarasota, Fl) microelectrode (pulled (Sutter, Novato, CA) to 6 to 9 MΩ when filled with 3M NaCl), amplified 1000× (WPI, Sarasota, Fl and Warner, Hamden, CT), and digitized (National Instruments, Austin, Texas) at 10 kHz using winLTP-version 2.4(Anderson and Collingridge, 2001)to follow fEPSP slope (averaged over 4 EPSPs), measured using 20% to 80% rise times, expressed as percent of baseline, during the course of an experiment. In order to be sure only “healthy” slices were included in our studies, responses had to meet several criteria: fiber volleys less than 1/3 of response amplitude and peak responses larger than 0.6 mV; responses and fiber volley must be stable (<5% drift). Following baseline stabilization of fEPSP slope at approximately 75% of maximal slope for at least 30 min, mGluR-LTD was induced using 900 paired-pulse stimuli at 1 Hz with 50 ms inter-pulse interval, SPP-LFS. D-APV (50 μM) or D,L-APV (100 μM) (Tocris, Ellisville, MO) was included in all experiments to block NMDA receptor mediated LTD, in order to insure mGluR-LTD was being isolated. It has been demonstrated in rats that using 50 ms inter-pulse interval facilitates mGluR-LTD (Kemp et al., 2000); in our prior work, mGluR-LTD induction was completely blocked by the mGluR5 specific antagonist MTEP (500 nM) (Bernard et al., 2013). Dead volume was kept to a minimum (9–10 mL) and flow rate was always tightly controlled (2–3 mL/min).

Where indicated, slices were incubated in isradipine (10 μM for 30 mins prior to and during recording, Tocris, Ellisville, MO), tatCN21 (2 μM for 40 mins prior to and during recording, Bayer lab), MG132 (10 μM for 30 mins prior to and during recording, Tocris, Ellisville, MO), PF-4708671 (25 μM for 30 min prior to and during recording, Tocris, Ellisville, MO) rapamycin (20 nM for 30 mins prior to and during recording, Tocris, Ellisville, MO) or U0126 (5 μM for 30 mins prior to and during recording, Tocris, Ellisville, MO). MG-132 and U0126 were dissolved in dimethyl sulfoxide (DMSO, 90 mM), while isradipine, PF-4708671 and rapamycin were dissolved in 40 mM DMSO. During these experiments, interweaved naïve mGluR-LTD experiments (i.e. vehicle, no inhibitor, Figure 2) were conducted in equal concentrations of DMSO. ACSF contained less than 0.0003% DMSO. We did not detect any effect of DMSO vehicle alone, therefore we included these experiments in naïve mGluR-LTD experiments shown in Figure 3. All statistical comparisons were performed using the average of responses obtained between the 65 and 75 minute time-points (50 to 60 minutes following the end of paired pulse stimulations).

Western blotting

Hippocampal slices were prepared and recovered as for electrophysiology with the addition of cuts to isolate CA1 from the remaining hippocampus; after recovery, the slices were suspended in STE buffer, sonicated, boiled for 5 minutes and then frozen until further use. In order to minimize the effects of slice preparation (Osterweil et al., 2010) and to control for slice quality, only slices that came from a preparation that met electrophysiological criteria were used. All concentrations were quantified with BCA and then loaded in duplicate on 10% polyacrylamide gel and a five-point dilution series of naive rat hippocampal homogenate was included on each gel as a standard curve for quantification of immunoreactivity/ μg loaded protein (Grosshans and Browning, 2001). Following transfer to PolyScreen PVDF transfer membrane (Genie, Idea Scientific Company, Minneapolis, MN, USA), blots were blocked in BSA or Carnation nonfat dry milk for 1 h and incubated either 1h at room temperature or overnight at 4 °C with antibodie s (Table 1). Blots were then subjected to three 10-min washings in Tris-buffered saline (140 mm NaCl, 20 mm Tris pH 7.6) plus 0.1% Tween 20 (TTBS), before being incubated with anti-mouse or anti-rabbit secondary antibody (1:5000) in 1% BSA or milk for 1 h at room temperature, followed by three additional 10-min washes preformed with TTBS. Immunodetection was accomplished using a chemiluminescent substrate kit (SuperSignal West Femto Maximum Sensitivity Substrate; Pierce) and the Alpha Innotech (Alpha Innotech, San Leandro, CA, USA) imaging system. Quantification was performed using AlphaEase software (Alpha Innotech, San Leandro, CA, USA) and Excel (Microsoft, Redmond, WA, USA). Immunoreactivity was reported as the density of sample bands relative to the standard curve. For phospho-proteins, ratios of immunoreactivity/ μg to totals are reported without standardization. Only values falling within the standard curve generated from the dilution series included on each gel were incorporated into the final analysis. Some of the blots were then stripped (Restore PLUS Western Blot Stripping Buffer; Thermo Scientific, Rockford, IL) and reblotted if needed.

Subcellular fractionation

Hippocampal slices were prepared and recovered as for electrophysiology and western blotting with the addition of cuts to isolate CA1 from the remaining hippocampus; after recovery, slices were placed in ice-cold buffered sucrose solution (50μL per slice) containing 320mM sucrose, 10mM Tris (pH 7.4), 40mM NaF, 300 nM okadaic acid, 1mM EDTA and 1mM EGTA. Slices were immediately homogenized in a glass grinding vessel by Teflon pestle rotating at 1000 RPM. Homogenates were then centrifuged at 1000×g for 10min. The pellet (P1), which contains nuclei and incompletely homogenized cells, was suspended (200μL 1× STE), sonicated and boiled for 5min at 100°C. The supernatant (S1) was centrifuged at 10,000×g for 15min. The pellet (P2), which contains synaptosomal plasma membrane, was suspended in 50 μL of 1× STE, sonicated and boiled. The supernatant (S2), which contains the soluble fraction, was precipitated with cold Acetone (4×) for at least 12h at −20°C, centrifuged at 15,000×g for 10min, air dried, suspended in 30μL of 1× STE, sonicated and boiled. Protein concentrations were quantified with BCA and then kept frozen until further semi-quantitative analysis as performed for western blotting.

Statistics

Data are expressed as mean ± SEM with n = number of rats for a given treatment. Data are plotted using Sigmaplot 12.0 (Systat, Chicago, IL). ,ANOVA (Holm-Sidak post-hoc testing) and Student's t-tests were used, where indicated and appropriate using SigmaPlot 12.0 (Systat, Chicago, IL). If statistical assumptions for a t-test were not met, we employed the Mann-Whitney Rank Sum test. Significance is reported at $P < 0.05$ unless otherwise stated.

Results

Comprehensive screening of mGluR-LTD related proteins in ELS rats

Upon determining that mGluR-LTD is significantly enhanced in adult ELS rats, we speculated that this exaggerated mGluR-LTD was the result of altered protein expression and/or phosphorylation. Theoretically, enhanced mGluR-LTD could be influenced by a number of proteins associated with mGluR post-synaptic signaling; therefore we assessed changes in the expression and phosphorylation state of numerous mGluR-LTD related proteins. The initial changes we detected were reported in (Bernard et al., 2013). A list of additional mGluR-LTD proteins assessed and results obtained are presented in Table 2 with further discussion of significant findings presented below. These specific proteins were selected as they are targets of phosphatases or kinases that are altered in the ELS model or because they are potentially associated with the cellular mechanisms of mGluR-LTD. Notably, we do not see alterations in the phosphorylation status of GluA1 or GluA2, often the down-stream targets of kinases and phosphatases that ultimately mediate synaptic plasticity. Expression of neuroligin 3 was reduced in ELS rats. Mutations in neuroligin 3 have been associated with autism (Jamain et al., 2003), supporting our previous hypothesis (Bernard et al., 2013) that ELS animals demonstrate changes similar to those associated with autism.

Altered phosphorylation of CaMKII

Synaptic plasticity is altered in the ELS model (Cornejo et al., 2007; Bernard et al., 2013) and CaMKII is involved in synaptic plasticity (Coultrap and Bayer, 2012; Mockett et al., 2011). Therefore we assessed total CaMKIIα and β, as well as their levels of phosphorylation at two distinct sites: T286 (T287 in CaMKIIβ), which induces Ca2+-independent "autonomous" CaMKII activity, and T305 (T306 in CaMKIIβ), which instead prevents activation by interfering with Ca2+/CaM binding. We detected no persistent changes in expression of CaMKIIα (control: 100.00 ± 15.90%, n = 12, ELS: 84.90 ± 13.80%, n = 11, P = 0.485, Student's t-test) or CaMKIIβ following ELS (control: 100.00 ± 9.06%, n = 9, ELS: 106.60 ± 16.10%, n = 12, P = 0.644, Student's t-test), (Figure 1). We detected no increase in phosphorylation of the CaMKII site T305 (control: 100.00 ± 18.89%, n = 12, ELS: 95.13 ± 25.22%, n = 13, P = 0.575, Student's t-test). However we detected significant increases in phosphorylation of site T286/7 on both CaMKIIα (control: 100.00 ± 27.74%, n = 9, ELS: 660.84 ± 182.85%, n = 8, P < 0.001, Student's t-test) and CaMKIIβ (control: 100.00 ± 27.50%, n = 9, ELS: 1213.33 ± 262.78%, n = 11, P < 0.05, Student's t-test). The specific phosphorylation profile of CaMKII following ELS is noteworthy. Isolated phosphorylation at T286 but not at T305 indicates that CaMKII was autonomously activated but still capable of further stimulation by CaM (Coultrap et al., 2010; Miller and Kennedy, 1986). This indicates that CaMKII is in an optimally primed state in ELS rats: its autonomous activity is persistently increased, yet activation levels can be driven even higher due to lack of increased phosphorylation at T305.

We further probed altered CaMKII phosphorylation in synaptic and cytosolic fractions (Figure 2). No significant changes were detected with respect to total CaMKIIa (control P2: 100.00 ± 43.60%, n = 9, ELS P2: 119.10 ± 24.70%, n = 7, P = 0.686, Mann-Whitey Rank Sum) (control S2: 100.00 ± 11.40%, n = 9, ELS S2: 95.40 ± 12.00%, n = 9, P = 0.785, Student's t-test) or CaMKIIβ (control P2: 100.00 ± 20.29%, n = 7, ELS P2: 105.22 ± 11.68%, n = 9, P = 0.817, Student's t-test) (control S2: 100.00 ± 11.23%, n = 9, ELS S2: 84.42 ± 8.83%, n = 9, P = 0.251, Mann-Whitey Rank Sum). CaMKIIα P-T286 was significantly elevated in the P2 fraction (control P2: 100.00 ± 18.00%, n = 7, ELS P2: 177.40 ± 27.20%, n = 9, P < 0.05, Student's t-test), but not in the S2 fraction (control S2: 100.00 ± 16.40%, n = 11, ELS S2: 138.70 ± 35.50%, n = 12, P = 0.474, Student's t-test). Mimicking this trend, CaMKIIβ P-T287 was significantly elevated in the P2 fraction (control P2: 100.00 ± 11.60%, n = 7, ELS P2: 180.76 ± 23.88%, n = 7, P < 0.02, Student's t-test), but not in the S2 fraction (control S2: 100.00 ± 18.40%, n = 7, ELS S2: 103.75 ± 28.69%, n = 9, P = 0.908, Mann-Whitey Rank Sum). This indicates that CaMKII is in an activated and optimally primed state selectively in synapses.

mGluR-LTD is permanently enhanced following ELS

We previously reported enhanced mGluR-LTD in adult ELS rats (Bernard et al., 2013). In order to insure that our ability to detect this phenomenon persisted, we interweaved additional ELS mGluR-LTD experiments with those that follow. These results confirmed our previous reports of enhanced mGluR-LTD in adult ELS rats (control: 80.32 ± 1.56%, n = 18, ELS: 53.50 ± 3.99%, n = 18, P < 0.0000004, Student's t-test) (Figure 3A and Figure

7). mGluR-LTD induction following ELS is completely blocked both by either the mGluR5 antagonist MTEP or protein synthesis inhibitors (Bernard et al., 2013).

Role of CaMKII in mGluR-LTD induction

CaMKII is traditionally associated with long term potentiation (Malenka and Bear, 2004; Coultrap and Bayer, 2012; Malinow et al., 1989; Silva et al., 1992). However recent evidence suggests CaMKII is also crucial for the induction of mGluR-LTD (Mockett et al., 2011), although the CaMKII inhibitors used in that study (KN62, KN93 and AIP) have off target effects, including VGCCs (Coultrap et al., 2011). We used a very selective CaMKII inhibitor, the peptide tatCN21 (2 mM), to specifically inhibit CaMKII activity (Vest et al., 2007). This concentration did not affect basal transmission (not shown). TatCN21 inhibits stimulated and autonomous CaMKII activity with the same potency (Buard et al., 2010). mGluR-LTD in the presence of tatCN21 is differentially affected in ELS versus control rats (control: 93.72 ± 1.31%, n = 11, ELS: 68.39 ± 1.98%, n = 10, $P < 0.001$, Student's t-test). TatCN21 significantly blocked mGluR-LTD in controls (control without CN21: 80.32 ± 1.56%, n = 18, controls with tatCN21: 93.72 ± 1.31%, n = 11, $P < 0.000003$, Student's t-test) (Figures 3AB and 7). However a small amount of mGluR-LTD was still induced in controls in the presence of tatCN21 (control baseline with tatCN21: 100.67 ± 1.04%, n = 11, controls with tatCN21: 93.72 ± 1.31%, n = 11, $P < 0.0003$, Student's t-test). mGluR-LTD in the presence of tatCN21 was still enhanced in ELS rats compared to control mGluR-LTD (control without tatCN21: 80.32 ± 1.56%, n = 18, ELS with tatCN21: 68.39 ± 1.98%, n = 10, $P < 0.001$, Student's t-test) (Figures 3AB and 7). However a small reduction of mGluR-LTD occurs in ELS rats in the presence of tatCN21 (ELS without tatCN21: 53.498 ± 3.99%, n = 18, ELS with tatCN21: 68.39 ± 1.98%, n = 10, $P < 0.05$, Student's t-test) (Figures 3AB and 7). These findings confirm with greater selectivity the previous reports that CaMKII activity is required for mGluR-LTD induction (Mockett et al., 2011). However the dependence of mGluR-LTD induction on CaMKII signaling was substantially reduced following ELS, which also display elevated basal levels of CaMKII activation prior to mGluR-LTD induction (Figure 1).

S6K regulation of mGluR-LTD is occluded following ELS

We have reported alterations in S6K signaling in the ELS model (Bernard et al., 2013), specifically S6K is overall activated or hyperphosphorylated following ELS selectively in synaptic fractions. S6K is implicated in the induction of mGluR-LTD (Ceman et al., 2003; Narayanan et al., 2007; Bassell and Warren, 2008; Narayanan et al., 2008). In order to determine if this role is altered following ELS we induced mGluR-LTD in the presence of an S6K inhibitor (PF-4708671, 25 μM) (Pearce et al., 2010). PF-4708671 completely blocked mGluR-LTD in controls (controls with PF-4708671: 106.14. ± 9.71%, n = 6; controls without PF-4708671: 80.32 ± 1.56%, n = 18, $P<0.001$) (Figures 4A, 3A and 7), yet mGluR-LTD was still equivalently present in ELS rats (ELS without PF-4708671: 53.50 ±3.99%, n = 18; ELS with PF-4708671: 54.96±8.75%, n = 10, $P = 0.864$, Student's t-test (Figures 4A, 3A and 7). In the presence of PF-4708671 ELS rats display significantly more mGluR-LTD (ELS with PF-4708671: 54.96±8.75%, n = 10; Control with PF-4708671: 106.14±9.71%, n = 6, $P = 0.002$, Student's t-test). These results confirmed that S6K signaling facilitates mGluR-LTD under control conditions and consistent with prior reports,

but S6K regulation of mGluR-LTD induction was completely lost following ELS. Similar to our findings with CaMKII, this is consistent with our prior findings of elevated levels of synaptic S6K activation (Bernard et al., 2013).

Role of Proteasome in mGluR-LTD induction

Proteasome mediated degradation of FMRP is a necessary process in mediating mGluR-LTD in adult rodents (Hou et al., 2006), while in younger rodents its role may be different (Citri et al., 2009). In order to determine if this process is still intact following ELS, we induced synaptic mGluR-LTD in the presence of MG-132 (10 μM), a proteasome inhibitor (control: 99.93 ± 6.05%, n = 8, ELS: 62.93 ± 7.83%, n = 6, P = 0.0025, Student's t-test) (Figure 4B). We confirmed earlier reports that proteasome mediated degradation is required to induce mGluR-LTD (control without MG 132: 80.32 ± 1.56%, n = 18, control with MG-132: 99.93 ± 6.05%, n = 8, P = 0.002, Mann-Whitey Rank Sum) (Figures 4B, 3A and 7). However following ELS, the requirement of proteasome mediated degradation, presumably of FMRP (Hou et al., 2006), was completely lost (ELS without MG 132: 53.50 ± 3.99%, n = 18, ELS: 62.93 ± 7.83%, n = 6, P = 0.484, Mann-Whitey Rank Sum) (Figures 4B, 3A and 7). This was consistent, as we have demonstrated that FMRP sub-cellular location and signaling is altered following ELS (Bernard et al., 2013), though other proteins important for mGluR-LTD may also be targeted for degradation.

Role of Voltage Gated Calcium channels in mGluR-LTD induction

The involvement of CaMKII in mGluR-LTD implies that a calcium source is required to activate CaMKII. Prior studies suggestively ruled out phospholipase-C, and thus release of calcium from internal stores (Mockett et al., 2011). In order to identify the calcium source for mGluR-LTD, we induced synaptic mGluR-LTD in the presence of the L-type VGCC blocker, isradipine (Ruegg and Hof, 1990; Striessnig et al., 1998). mGluR-LTD was completely occluded in control rats in the presence of isradipine (10 μm), while mGluR-LTD was partially occluded in ELS rats (control with isradipine: 100.44 ± 4.70%, n = 5, ELS with isradipine: 75.67 ± 5.26%, n = 9, P < 0.009, Student's t-test)(control without isradipine: 80.23 ± 1.56%, n = 18, control with isradipine: 100.439 ± 4.691%, n = 5, P < 0.001, Student's t-test)(ELS without isradipine: 53.50 ± 3.99%, n = 18, ELS with isradipine 75.67 ± 5.26%, n = 9, P < 0.005) (Figures 5A, 3A and 7). It is noteworthy that blocking voltage gated calcium channels with isradipine normalized mGluR-LTD in ELS rats compared to naïve controls (control mGluR-LTD without isradipine; 80.23 ± 1.56%, n = 18, ELS with isradipine: 75.67 ± 5.26%, n = 9, P = 0.287, Student's t-test) (Figures 5A, 3A and 7). Taken together, VGCCs are required for mGluR-LTD induction and may underlie the calcium source for CaMKII activation, however the necessity for VGCCs (and CaMKII) for mGluR-LTD induction is lost following ELS.

Involvement of the mTOR pathway in mGluR-LTD induction

The mTOR pathway is widely implicated as necessary for mGluR-LTD induction (Bassell and Warren, 2008; Ceman et al., 2003; Narayanan et al., 2007; Narayanan et al., 2008). However, increased mGluR-LTD in ELS rats persisted in the presence of rapamycin (20 nM)(control: 96.71 ± 2.45%, n = 7, ELS: 58.09 ± 7.20%, n = 5, P < 0.0002, Student's t-test) (Figure 5B). As expected, rapamycin completely inhibited mGluR-LTD in control rats)

(control without rapamycin: 80.23 ± 1.56%, n = 18, control with rapamycin: 96.71 ± 2.45%, n = 7, P < 0.001, Student's t-test), indicating the mTOR pathway was a necessary component of mGluR-LTD. The requirement for mTOR activation during mGluR-LTD induction was lost in ELS rats (ELS without rapamycin: 53.50 ± 3.99%, n = 18, ELS with rapamycin: 58.09 ± 7.20%, n = 5, P = 0.831, Mann-Whitey Rank Sum) (Figures 5B, 3A and 7). Our prior results did not find activation of AKT, upstream of mTOR, but did find activated S6K, downstream of mTOR (Bernard et al., 2013). Presumably, activation of S6K removes the necessity of mTOR activation to mediate mGluR-LTD induction. However, taken together with our other findings, pre-activation of multiple kinases results in the loss of necessity of mTOR activation to mediate mGluR-LTD induction.

Altered phosphorylation of ERK following ELS

ERK phosphorylation has been implicated in both increased (Gallagher et al., 2004) and decreased (Chevere-Torres et al., 2012) mGluR-LTD. Expression of ERK was not significantly altered in ELS rats (control: 100.00 ± 29.05%, n = 11, ELS: 113.97 ± 22.50%, n = 11, P = 0.707, Student's t-test) (Figure 6A). However, phosphorylation of ERK was significantly and substantially reduced in ELS rats (control: 100.00 ± 34.12%, n = 7, ELS: 28.88 ± 8.52%, n = 8, P < 0.05, Student's t-test) (Figure 6B), suggesting ERK signaling may be involved in altered mGluR-LTD following ELS.

MEK/ERK 1/2 involvement in mGluR-LTD induction

MEK/ERK 1/2 has been implicated in mGluR-LTD (Banko et al., 2006; Chevere-Torres et al., 2012; Gallagher et al., 2004; Osterweil et al., 2010) therefore we used U0126, a MEK/EKR 1/2 inhibitor, to block MEK/ERK 1/2 activity to see if its role in mGluR-LTD is altered in the ELS model. In contrast to the prior experiments, we did not find a significant difference between ELS and control mGluR-LTD in the presence of U0126 (control: 46.97 ± 9.56%, n = 7, ELS: 68.77 ± 6.06%, n = 7, P < 0.08, Student's t-test) (Figure 6C). Blocking MEK/ERK activity enhanced mGluR-LTD in control rats (control without U0126: 80.32 ± 1.56%, n = 18, control with U0126: 46.97 ± 9.56%, n = 7, ELS: P < 0.01, Mann-Whitey Rank Sum) (Figures 3A, 6C and 7). In the presence U0126, control rats displayed levels of mGluR-LTD, similar to that observed in ELS rats in naïve conditions (ELS without U0126: 53.50 ± 3.99%, n = 18, control with U0126: 46.97 ± 9.56, n = 7, P = 0.459, Student's t-test) (Figures 3A, 6C and 7). Blocking MEK/ERK activity had the opposite effect on mGluR-LTD in ELS rats, it slightly blocked mGluR-LTD (ELS without U0126: 53.50 ± 3.99%, n = 18, ELS with U0126: 68.77 ± 6.06%, n = 7, P = 0.05) (Figures 2A, 5C and 6). Taken together with altered ERK phosphorylation (Figure 6AB), this suggests that MEK/ERK pathway signaling was functionally altered in ELS rats.

Discussion

Our ELS model is distinct from other early life seizure models, as it does not result in spontaneous recurrent seizures (Bernard et al., 2013). Furthermore, in the hippocampus, there are no anatomical changes (cell loss, synaptic reorganization, spine numbers) or changes in basal neural transmission (Cornejo et al., 2007). Despite lack of overt changes, ELS animals have behavioral deficits in learning/memory and social tasks (Bernard et al.,

2013; Cornejo et al., 2007; Cornejo et al., 2008). These findings led to the exploration of synaptic plasticity and related cell signaling pathways. We have reported selectively enhanced mGluR-LTD (NMDAR-LTD is unaffected) that is still protein synthesis dependent. We suspect changes in mGluR-LTD are responsible for behavioral deficits following ELS (Bernard et al., 2013). Many of these findings mimic the behavioral and mGluR-LTD changes in the FMRP KO mouse, although mGluR-LTD in the FMRP KO is no longer protein synthesis dependent (Nosyreva and Huber, 2006).

Prior work demonstrated that the FMRP/PP2A/S6K complex is altered in ELS rats, correlating with unchecked mGluR-LTD (Bernard et al., 2013). Specifically, S6K is unbound from the complex and S6K is hyperphosphorylated, specifically at synapses. We further explored changes to the PP2A/FMRP/S6K “brake” on protein synthesis by inducing mGluR-LTD in the presence of the S6K inhibitor PF-4708617. These results provide further support for our previous conclusions that the PP2A/FMRP/S6K “brake” on protein synthesis is “broken” in ELS rats and partly mediated by S6K. The S6K inhibitor blocked mGluR-LTD in control rats, yet had no effect in ELS rats, indicating that the influence that the PP2A/FMRP/S6K complex exerts over mGluR-LTD is disrupted. Our results also support the concept that rephosphorylation of FMRP by S6K is a crucial step in mediating mGluR-LTD in the normal state. Under the current schema, S6K action is bimodal to both activate translation via S6 and to rephophorylate FMRP, causing FMRP to attach to the ribosome, thus reinstalling the brake on protein synthesis and mGluR-LTD (Bassell and Warren, 2008; Ceman et al., 2003; Narayanan et al., 2007; Narayanan et al., 2008; Sharma et al., 2010). These results are therefore cautiously interpreted mechanistically, as two opposing functions of S6K are likely blocked by the S6K inhibitor.

We then sought to disrupt the mGluR-AKT-mTOR-S6K pathway upstream of S6K by blocking mTOR activity with rapamycin. Given the current schema, we expected rapamycin to fully inhibit mGluR-LTD following ELS as well as in controls, as previously shown (Hou and Klann, 2004; Potter et al., 2013; Sharma et al., 2010), as mTOR is responsible for activating protein synthesis (Sharma et al., 2010) and also for limiting protein synthesis (Tang et al., 2002). Our results in ELS rats were contrary to what was expected. mGluR-LTD in the ELS model was rapamycin insensitive, similar to what is found in the FMRP KO mouse (Sharma et al., 2010). However the mechanism by which mTOR fails to block mGluR-LTD in each of these models is likely different, as mGluR-LTD is protein synthesis dependent in the ELS model (Bernard et al., 2013) and protein synthesis independent in the FMRP KO (Nosyreva and Huber, 2006). mTOR may also influence mGluR-LTD related protein synthesis via other downstream targets. This supports multiple, redundant pathways to activate mGluR-LTD associated protein synthesis.

Proteasome mediated degradation of FMRP is a crucial step in the induction of mGluR-LTD. Blocking this process blocks mGluR-LTD in wild type rats, but has no effect in FMRP KOs (Hou et al., 2006), supporting the role of FMRP degradation in mGluR-LTD induction. Our results in control rats support previous findings, by demonstrating that blocking proteasome mediated protein degradation blocked mGluR-LTD and confirming that proteasome mediated degradation, presumably of FMRP, was a crucial step in mediating mGluR-LTD. MG-132 had minimal effect on mGluR-LTD in ELS rats, similar to what is

observed in the FMRP KO. We have detected abnormal sub-cellular distribution of FMRP in ELS rats, away from the cytosolic compartment (Bernard et al., 2013). Therefore the loss of the impact of FMRP degradation on mGluR-LTD is not surprising and our data suggests that cytosolic FMRP may be the target of mGluR-LTD related degradation.

ERK and mTOR signaling are thought to function independently to control mGluR-LTD related protein synthesis via different signaling pathways (Osterweil et al., 2010), suggesting alterations in ERK and mTOR could independently contribute to enhanced mGluR-LTD. Our finding of reduced ERK phosphorylation in conjunction with enhanced mGluR-LTD following ELS is in agreement with previous reports from a TSC model that demonstrates increased phosphorylation of ERK in combination with reduced mGluR-LTD. Further, blocking ERK activity with UO126 rescues mGluR-LTD in a TSC model (Chevere-Torres et al., 2012). Taken together these findings strongly implicate enhanced ERK signaling in restricting mGluR-LTD. Altered ERK signaling in the ELS model correlates with our previous report of altered levels of striatal-enriched protein tyrosine phosphatase (STEP) in these rats (Bernard et al., 2013). STEP dephosphorylates ERK, preventing its nuclear translocation and subsequent nuclear signaling (Paul et al., 2003). STEP translation is triggered by group I mGluRs and subsequent activation of the ERK, PI3K and mTORC1 pathways (Zhang et al., 2008). Therefore it is possible that enhanced STEP expression in ELS rats (Bernard et al., 2013), which is associated with enhanced mGluR-LTD (Moult et al., 2006; Zhang et al., 2008), may influence altered ERK signaling.

Our results suggest that ERK's influence on mGluR-LTD is complex. While blocking ERK enhanced mGluR-LTD in controls, it slightly suppressed it in ELS rats. This could indicate that there are multiple downstream targets of ERK. Some function to increase mGluR-LTD, others to limit it. Working from this schema, our results indicate that ERK's ability to enhance mGluR-LTD is lost following ELS, yet its ability to limit mGluR-LTD is intact. It is also possible that ERK phosphorylation acts as a dynamic indicator of recent mGluR activity that may influence the amount of mGluR-LTD. In ΔRG mice (a TSC model), robust enhancement of ERK signaling results in impaired mGluR-LTD (Chevere-Torres et al., 2012), whereas modest activation of ERK and mTORC1 signaling in FXS model mice results in enhanced mGluR-LTD (Hou et al., 2006; Potter et al., 2013; Sharma et al., 2010).

Increased phosphorylation at T286 and lack of increased phosphorylation at T305 (Figure 1) indicates that CaMKII is in an optimal activation state exclusively at synapses (Figure 2). Phosphorylation at T286 results in autonomous CaMKII activity, while unchanged T305 phosphorylation allows CaMKII activity to be further elevated via increases in intracellular calcium. Our data extend prior reports (Mockett et al., 2011) by showing the dependence of mGluR-LTD induction on CaMKII using a more specific inhibitor. Blocking CaMKII activity with tatCN21 significantly blocked mGluR-LTD induction in control rats. While a minimal amount of mGluR-LTD is still induced in control rats in the presence of tatCN21, it is minimal and very different than in the absence of tatCN21.

Results with tatCN21 in ELS rats demonstrated that acute activation of CaMKII was no longer required to induce mGluR-LTD (Figure 3). We speculate that due to persistently elevated CaMKII activity in ELS rats, CaMKII has already phosphorylated the required

substrates to facilitate mGluR-LTD prior to induction. Therefore even in the presence of a CaMKII inhibitor, mGluR-LTD can occur. Typical substrates associated with CaMKII signaling (Table 2) were not affected in ELS rats. It is suggested that there are unidentified substrates that may be involved in the control of protein synthesis (see (Mockett et al., 2011)), one attractive target is the proteasome (Bingol et al., 2010; Djakovic et al., 2009; Jarome et al., 2013). Elevated autonomous CaMKII, as detected in ELS rats, activates the proteasome and this may facilitate FMRP degradation, resulting in enhanced mGluR-LTD (Hou et al., 2006).

The involvement of CaMKII in mGluR-LTD as demonstrated here and by others (Mockett et al., 2011) implicates the importance of a calcium source in mediating mGluR-LTD. However the identity of the calcium source for mGluR-LTD was not previously determined (Mockett et al., 2011). We have now demonstrated that calcium influx via L-type VGCCs was a necessary aspect of mGluR-LTD induction in control rats. In the naïve, control state, we speculate that calcium influx via L-type VGCCs (during mGluR-LTD induction) activated CaMKII and CaMKII proceeded to phosphorylate substrates needed to facilitate mGluR-LTD, presumably to regulate protein synthesis. Results in ELS rats indicate that influx of calcium via L-type VGCCs was no longer required for mGluR-LTD induction. Further, blockade of L-type calcium channels had the largest effect in ELS rats compared to other inhibitors. In ELS rats, given the “autonomous” state of CaMKII, as indicated by elevated phosphorylation at T286 (and lack of increased phosphorylation at T305/306), L-type calcium channels speculatively mediate calcium accumulations that may further stimulate CaMKII to mediate exaggerated mGluR-LTD induction in ELS rats. However it is equally plausible to invoke other calcium-mediated processes, presentation of CaMKII substrates with mGluR-LTD induction that do not require maximally stimulated CaMKII, or prior phosphorylation of substrates by “autonomous” CaMKII. The persistent phosphorylation of these substrates may reduce the need for CaMKII and L-type VGCC activation at the time of mGluR-LTD induction. Determining the magnitude of calcium accumulations necessary to trigger mGluR-LTD, and thus regulate CaMKII activity and perhaps the amount of mGluR-LTD, is an area for further study. The temporal profile of VGCC activation, subsequent calcium accumulation and CaMKII activation may also be crucial in determining the extent of synaptic plasticity as has been shown for LTP and NMDAR-LTD (Malenka and Bear, 2004).

In summary, multiple pathways converge upon mGluR-LTD associated protein synthesis. These pathways include, but may not be limited to: mTOR, S6K, the proteasome, L-type VGCCs and CaMKII. While each may be necessary in order to induce mGluR-LTD under normal conditions, they appear to be insufficient independently. This implies that while these factors may normally act sequentially to mediate mGluR-LTD, this is no longer the case after ELS. If one or more of these pathways exists in a permanently altered state of activation, then the requirement for the involvement of each pathway is lost and excessive mGluR-LTD is readily induced. This can occur in known genetic disruptions, such as the FMRP KO, or in the ELS rat model here. These models mimic features of intellectual disability and autism spectrum disorder and our work implicates these pathways in these disorders, particularly activated CaMKII and L-type channels, which have never before been linked to these disorders.

Acknowledgments

Special thanks to Drs. Heather O'Leary, Mark Dell'Acqua, Steve Coultrap and other members of the Benke, Bayer and Dell'Acqua labs and the Neuroscience Program Machine Shop Core. Funding provided by the Children's Hospital Colorado Research Institute, Epilepsy Foundation, and National Institutes of Health grants R01 NS076577 (to T.B.) and R01 NS081248 (to K.U.B.). The content is solely the responsibility of the authors and does not necessarily represent the official views of NINDS or NIH.

Abbreviations

ACSF	artificial cerebral spinal fluid
APV	Amino-5-phosphonopentanoic acid CaMKII, Calcium-Calmodulin Kinase II
DMSO	dimethyl sulfoxide
ELS	early life seizure
fEPSP	Field excitatory post-synaptic potentials
ERK1/2	extracellular signal-regulated kinase 1/2
FMRP	Fragile X Mental Retardation Protein
MEK	Mitogen-activated protein kinase
mGluR	metabotropic glutamate receptor
mGluR-LTD	mGluR mediated long term depression
mTOR	mammalian target of rapamycin
PP2A	protein phosphatase 2A
S6K	S6 Kinase
STEP	striatal-enriched protein tyrosine Phosphatase
TSC	tuberous sclerosis complex
L-type VGCC	L-type voltage gated calcium channel.

References

Anderson WW, Collingridge GL. The LTP program: a data acquistion program for on-line analysis of long-term potentiation and other synaptic events. J Neurosci Methods. 2001; 108:71–83. [PubMed: 11459620]

Banko JL, Hou L, Poulin F, Sonenberg N, Klann E. Regulation of eukaryotic initiation factor 4E by converging signaling pathways during metabotropic glutamate receptor-dependent long-term depression. J Neurosci. 2006; 26:2167–2173. [PubMed: 16495443]

Bassell GJ, Warren ST. Fragile X syndrome: loss of local mRNA regulation alters synaptic development and function. Neuron. 2008; 60:201–214. [PubMed: 18957214]

Bernard PB, Castano AM, O'Leary H, Simpson K, Browning MD, Benke TA. Phosphorylation of FMRP and alterations of FMRP complex underlie enhanced mLTDmGluR-LTD in adult rats triggered by early life seizures. Neurobiol Dis. 2013; 59:1–17. [PubMed: 23831253]

Bingol B, Wang CF, Arnott D, Cheng D, Peng J, Sheng M. Autophosphorylated CaMKIIalpha acts as a scaffold to recruit proteasomes to dendritic spines. Cell. 2010; 140:567–578. [PubMed: 20178748]

Buard I, Coultrap SJ, Freund RK, Lee YS, Dell'Acqua ML, Silva AJ, Bayer KU. CaMKII "autonomy" is required for initiating but not for maintaining neuronal long-term information storage. J Neurosci. 2010; 30(24):8214–8220. [PubMed: 20554872]

Ceman S, O'Donnell WT, Reed M, Patton S, Pohl J, Warren ST. Phosphorylation influences the translation state of FMRP-associated polyribosomes. Hum Mol Genet. 2003; 12:3295–3305. [PubMed: 14570712]

Chevere-Torres I, Kaphzan H, Bhattacharya A, Kang A, Maki JM, Gambello MJ, Arbiser JL, Santini E, Klann E. Metabotropic glutamate receptor-dependent long-term depression is impaired due to elevated ERK signaling in the DeltaRG mouse model of tuberous sclerosis complex. Neurobiol Dis. 2012; 45:1101–1110. [PubMed: 22198573]

Citri A, Soler-Llavina G, Bhattacharyya S, Malenka RC. N-methyl-D-aspartate receptor- and metabotropic glutamate receptor-dependent long-term depression are differentially regulated by the ubiquitin-proteasome system. Eur J Neurosci. 2009; 30:1443–1450. [PubMed: 19821836]

Conn PJ, Pin JP. Pharmacology and functions of metabotropic glutamate receptors. Annu Rev Pharmacol Toxicol. 1997; 37:205–237. [PubMed: 9131252]

Cornejo BJ, Mesches MH, Benke TA. A single early-life seizure impairs short-term memory but does not alter spatial learning, recognition memory, or anxiety. Epilepsy Behav. 2008; 13:585–592. [PubMed: 18678283]

Cornejo BJ, Mesches MH, Coultrap S, Browning MD, Benke TA. A single episode of neonatal seizures permanently alters glutamatergic synapses. Ann Neurol. 2007; 61:411–426. [PubMed: 17323345]

Coultrap SJ, Bayer KU. CaMKII regulation in information processing and storage. Trends Neurosci. 2012; 35:607–618. [PubMed: 22717267]

Coultrap SJ, Buard I, Kulbe JR, Dell'Acqua ML, Bayer KU. CaMKII autonomy is substrate-dependent and further stimulated by Ca2+/calmodulin. J Biol Chem. 2010; 285:17930–17937. [PubMed: 20353941]

Coultrap SJ, Vest RS, Ashpole NM, Hudmon A, Bayer KU. CaMKII in cerebral ischemia. Acta Pharmacol Sin. 2011; 32:861–872. [PubMed: 21685929]

Dingledine R, Borges K, Bowie D, Traynelis SF. The glutamate receptor ion channel. Pharmacol Rev. 1999; 51:7–61. [PubMed: 10049997]

Djakovic SN, Schwarz LA, Barylko B, DeMartino GN, Patrick GN. Regulation of the proteasome by neuronal activity and calcium/calmodulin-dependent protein kinase II. J Biol Chem. 2009; 284:26655–26665. [PubMed: 19638347]

Dzhala VI, Talos DM, Sdrulla DA, Brumback AC, Mathews GC, Benke TA, Delpire EJ, Jensen FE, Staley KJ. NKCC1 transporter facilitates seizures in the developing brain. Nat Med. 2005; 11:1205–1213. [PubMed: 16227993]

Gallagher SM, Daly CA, Bear MF, Huber KM. Extracellular signal-regulated protein kinase activation is required for metabotropic glutamate receptor-dependent long-term depression in hippocampal area CA1. J Neurosci. 2004; 24:4859–4864. [PubMed: 15152046]

Gladding CM, Fitzjohn SM, Molnar E. Metabotropic glutamate receptor-mediated long-term depression: molecular mechanisms. Pharmacol Rev. 2009; 61:395–412. [PubMed: 19926678]

Grosshans DR, Browning MD. Protein kinase C activatio induces tyrosine phosphorylation of the NR2A and NR2B subunits of the NMDA receptor. J Neurochem. 2001; 76:737–744. [PubMed: 11158244]

Hay N, Sonenberg N. Upstream and downstream of mTOR. Genes Dev. 2004; 18:1926–1945. [PubMed: 15314020]

Hou L, Antion MD, Hu D, Spencer CM, Paylor R, Klann E. Dynamic translational and proteasomal regulation of fragile X mental retardation protein controls mGluR-dependent long-term depression. Neuron. 2006; 51:441–454. [PubMed: 16908410]

Hou L, Klann E. Activation of the phosphoinositide 3-kinase-Akt-mammalian target of rapamycin signaling pathway is required for metabotropic glutamate receptor-dependent long-term depression. J Neurosci. 2004; 24:6352–6361. [PubMed: 15254091]

Huber KM, Kayser MS, Bear MF. Role for rapid dendritic protein synthesis in hippocampal mGluR-dependent long-term depression. Science. 2000; 288:1254–1257. [PubMed: 10818003]

Jamain S, Quach H, Betancur C, Råstam M, Colineaux C, Gillberg C, Söderström H, Giros B, Leboyer M, Gillberg C, Bourgeron T. Mutations of the X-linked genes encoding neuroligins NLGN3 and NLGN4 are associated with autism. Nat Genet. 2013; 34(1):27–29. [PubMed: 12669065]

Jarome TJ, Kwapis JL, Ruenzel WL, Helmstetter FJ. CaMKII, but not protein kinase A, regulates Rpt6 phosphorylation and proteasome activity during the formation of long-term memories. Front Behav Neurosci. 2013; 7:115. [PubMed: 24009566]

Kemp N, McQueen J, Faulkes S, Bashir ZI. Different forms of LTD in the CA1 region of the hippocampus. role of age and stimulus protocol. 2000:360–366.

Klann E, Dever TE. Biochemical mechanisms for translational regulation in synaptic plasticity. Nat Rev Neurosci. 2004; 5:931–942. [PubMed: 15550948]

Kuenzi FM, Fitzjohn SM, Morton RM, Collingridge GL, Seabrook GR. Reduced long-term potentiation in hippocampal slices prepared using sucrose-based artificial cerebrospinal fluid. J Neurosci Methods. 2000; 100:117–122. [PubMed: 11040373]

Lisman J, Yasuda R, Raghavachari S. Mechanisms of CaMKII action in long-term potentiation. Nat Rev Neurosci. 2012; 13:169–182. [PubMed: 22334212]

Luscher C, Huber KM. Group 1 mGluR-dependent synaptic long-term depression: mechanisms and implications for circuitry and disease. Neuron. 2010; 65:445–459. [PubMed: 20188650]

Malenka RC, Bear MF. LTP and LTD: an embarrassment of riches. Neuron. 2004; 44:5–21. [PubMed: 15450156]

Malinow R, Schulman H, Tsien RW. Inhibition of postsynaptic PKC or CaMKII blocks induction but not expression of LTP. Science. 1989; 245:862–866. [PubMed: 2549638]

Miller SG, Kennedy MB. Regulation of brain type II Ca2+/calmodulin-dependent protein kinase C by autophosphorylation: a Ca2+-triggered molecular switch. Cell. 1986; 44:861–870. [PubMed: 3006921]

Mockett BG, Guevremont D, Wutte M, Hulme SR, Williams JM, Abraham WC. Calcium/Calmodulin-Dependent Protein Kinase II Mediates Group I Metabotropic Glutamate Receptor-Dependent Protein Synthesis and Long-Term Depression in Rat Hippocampus. J Neurosci. 2011; 31:7380–7391. [PubMed: 21593322]

Moult PR, Gladding CM, Sanderson TM, Fitzjohn SM, Bashir ZI, Molnar E, Collingridge GL. Tyrosine phosphatases regulate AMPA receptor trafficking during metabotropic glutamate receptor-mediated long-term depression. J Neurosci. 2006; 26:2544–2554. [PubMed: 16510732]

Nakanishi S. Metabotropic glutamate receptors: synaptic transmission, modulation, and plasticity. Neuron. 1994; 13:1031–1037. [PubMed: 7946343]

Narayanan U, Nalavadi V, Nakamoto M, Pallas DC, Ceman S, Bassell GJ, Warren ST. FMRP phosphorylation reveals an immediate-early signaling pathway triggered by group I mGluR and mediated by PP2A. J Neurosci. 2007; 27:14349–14357. [PubMed: 18160642]

Narayanan U, Nalavadi V, Nakamoto M, Thomas G, Ceman S, Bassell GJ, Warren ST. S6K1 phosphorylates and regulates fragile X mental retardation protein (FMRP) with the neuronal protein synthesis-dependent mammalian target of rapamycin (mTOR) signaling cascade. J Biol Chem. 2008; 283:18478–18482. [PubMed: 18474609]

Nosyreva ED, Huber KM. Metabotropic receptor-dependent long-term depression persists in the absence of protein synthesis in the mouse model of fragile X syndrome. J Neurophysiol. 2006; 95:3291–3295. [PubMed: 16452252]

Osterweil EK, Krueger DD, Reinhold K, Bear MF. Hypersensitivity to mGluR5 and ERK1/2 leads to excessive protein synthesis in the hippocampus of a mouse model of fragile X syndrome. J Neurosci. 2010; 30:15616–15627. [PubMed: 21084617]

Paul S, Nairn AC, Wang P, Lombroso PJ. NMDA-mediated activation of the tyrosine phosphatase STEP regulates the duration of ERK signaling. Nat Neurosci. 2003; 6:34–42. [PubMed: 12483215]

Pearce LR, Alton GR, Richter DT, Kath JC, Lingardo L, Chapman J, Hwang C, Alessi DR. Characterization of PF-4708671, a novel and highly specific inhibitor of p70 ribosomal S6 kinase (S6K1). Biochem J. 2010; 431:245–255. [PubMed: 20704563]

Pin J-P, Duvoisin R. The metabotropic glutamate receptors: Structure and functions. Neuropharmacol. 1995; 34:1–26.

Potter WB, Basu T, O'Riordan KJ, Kirchner A, Rutecki P, Burger C, Roopra A. Reduced juvenile long-term depression in tuberous sclerosis complex is mitigated in adults by compensatory recruitment of mGluR5 and Erk signaling. PLoS Biol. 2013; 11:e1001627. [PubMed: 23966835]

Ruegg UT, Hof RP. Pharmacology of the calcium antagonist isradipine. Drugs 40 Suppl. 1990; 2:3–9.

Sarbassov DD, Ali SM, Sabatini DM. Growing roles for the mTOR pathway. Curr Opin Cell Biol. 2005; 17:596–603. [PubMed: 16226444]

Sharma A, Hoeffer CA, Takayasu Y, Miyawaki T, McBride SM, Klann E, Zukin RS. Dysregulation of mTOR signaling in fragile X syndrome. J Neurosci. 2010; 30:694–702. [PubMed: 20071534]

Silva AJ, Stevens CF, Tonegawa S, Wang Y. Deficient hippocampal long-term potentiation in a-calcium- calmodulin kinase II mutant mice. Science. 1992; 257:201–206. [PubMed: 1378648]

Stefani G, Fraser CE, Darnell JC, Darnell RB. Fragile X mental retardation protein is associated with translating polyribosomes in neuronal cells. J Neurosci. 2004; 24:7272–7276. [PubMed: 15317853]

Striessnig J, Grabner M, Mitterdorfer J, Hering S, Sinnegger MJ, Glossmann H. Structural basis of drug binding to L Ca2+ channels. Trends Pharmacol Sci. 1998; 19:108–115. [PubMed: 9584627]

Tang SJ, Reis G, Kang H, Gingras AC, Sonenberg N, Schuman EM. A rapamycin-sensitive signaling pathway contributes to long-term synaptic plasticity in the hippocampus. Proc Natl Acad Sci U S A. 2002; 99:467–472. [PubMed: 11756682]

Tremblay E, Nitecka L, Berger ML, Ben-Ari Y. Maturation of kainic acid seizure-brain damage syndrome in the rat. I. Clinical, electrographic and metabolic observations. Neuroscience. 1984; 13:1051–1072. [PubMed: 6527789]

Vest RS, Davies KD, O'Leary H, Port JD, Bayer KU. Dual mechanism of a natural CaMKII inhibitor. Mol Biol Cell. 2007; 18:5024–5033. [PubMed: 17942605]

Zhang Y, Venkitaramani DV, Gladding CM, Zhang Y, Kurup P, Molnar E, Collingridge GL, Lombroso PJ. The tyrosine phosphatase STEP mediates AMPA receptor endocytosis after metabotropic glutamate receptor stimulation. J Neurosci. 2008; 28:10561–10566. [PubMed: 18923032]

Highlights

- Early life seizures (ELS) alter the induction mechanisms of mGluR-LTD in adult rats.
- S6K, mTOR, proteasome, CaMKII and L-type VGCCs are each necessary for mGluR-LTD.
- After ELS, these pathways are no longer required to induce mGluR-LTD.
- “Autonomous” CaMKII was upregulated synaptically after ELS.
- ERK/MEK activation regulates the amount of expression, not induction.

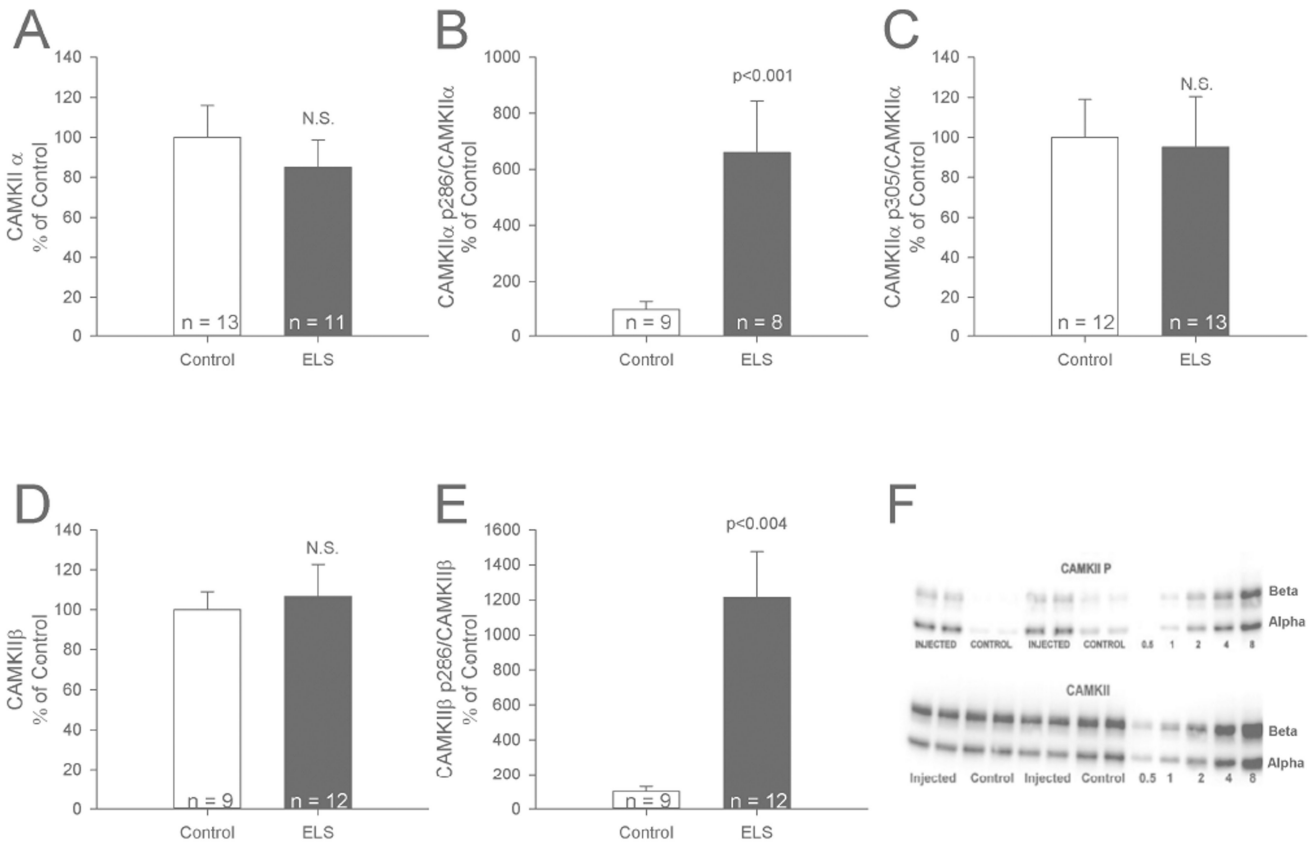

Figure 1. Increased phosphorylation of CaMKII following ELS

A, ELS caused no changes in expression of total CaMKIIα. B, ELS caused significant increases in phosphorylation of site T286 on CaMKIIα. C, ELS caused no changes in phosphorylation of the CaMKII site T305/6. D, ELS did not change total expression of CaMKIIβ. E, ELS caused significant increases in phosphorylation of site T287 on CaMKIIβ. F, example western blots for CaMKIIα T286. Semi-quantitative western-blot technique (Cornejo et al., 2007) was used to determine immunoreactivity/mg loaded protein, which were normalized to controls (see Methods).

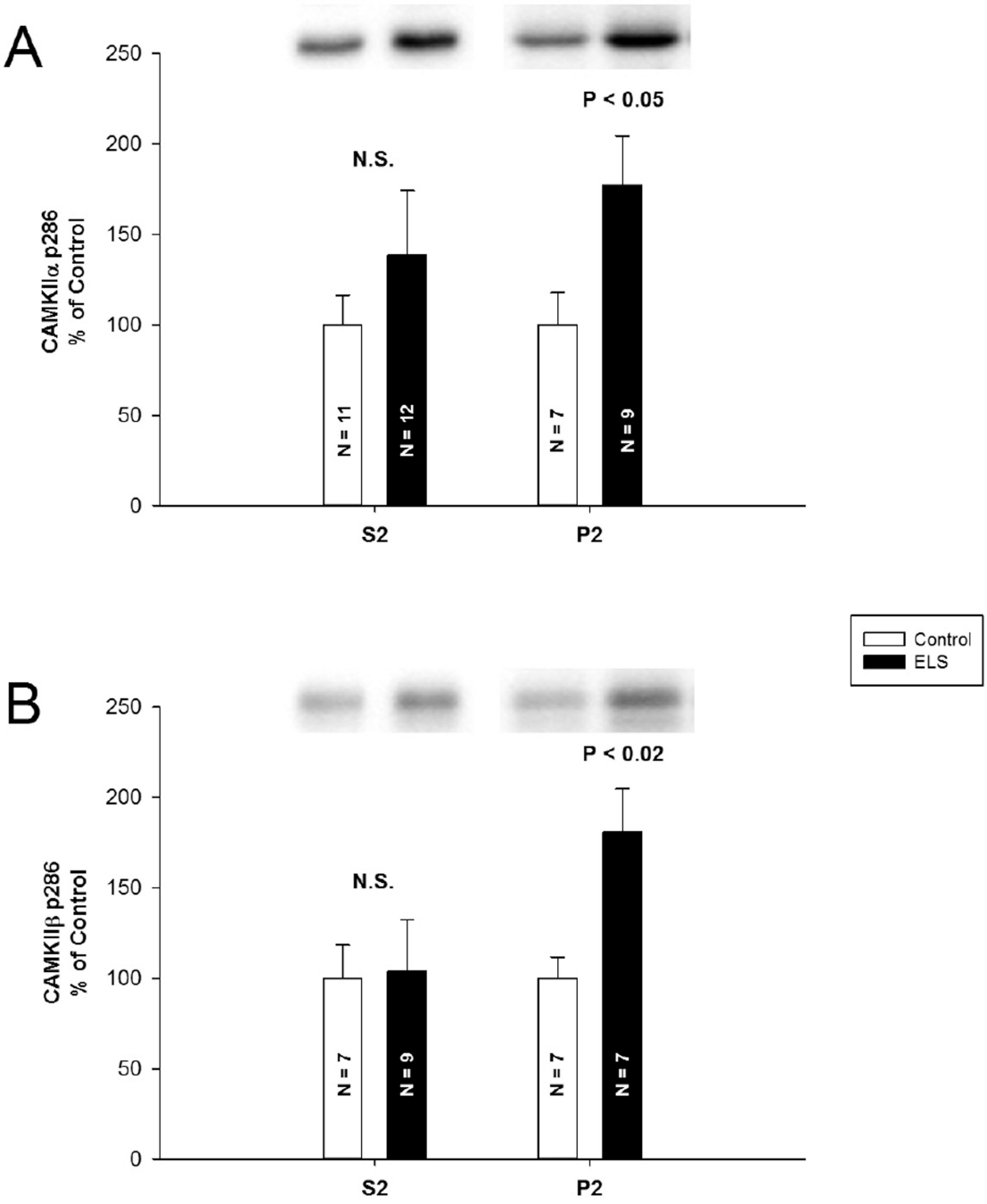

Figure 2. Increased phosphorylation of synaptic CAMKII

A, CaMKIIa P-T286 was significantly elevated in the P2 fraction (control P2: 100.00 ± 18.00%, n = 7, ELS P2: 177.40 ± 27.20%, n = 9, P < 0.05, Student's t-test), but not in the S2 fraction (control S2: 100.00 ± 16.40%, n = 11, ELS S2: 138.70 ± 35.50%, n = 12, P = 0.474, Student's t-test). B, mimicking this trend, CaMKIIβ P-T287 was significantly elevated in the P2 fraction (control P2: 100.00 ± 11.60%, n = 7, ELS P2: 180.76 ± 23.88%, n = 7, P < 0.02, Student's t-test), but not in the S2 fraction (control S2: 100.00 ± 18.40%, n = 7, ELS S2: 103.75 ± 28.69%, n = 9, P = 0.908, Mann-Whitey Rank Sum). Semi-quantitative western-

blot technique (Cornejo et al., 2007) was used to determine immunoreactivity/mg loaded protein, which were normalized to controls (see Methods).

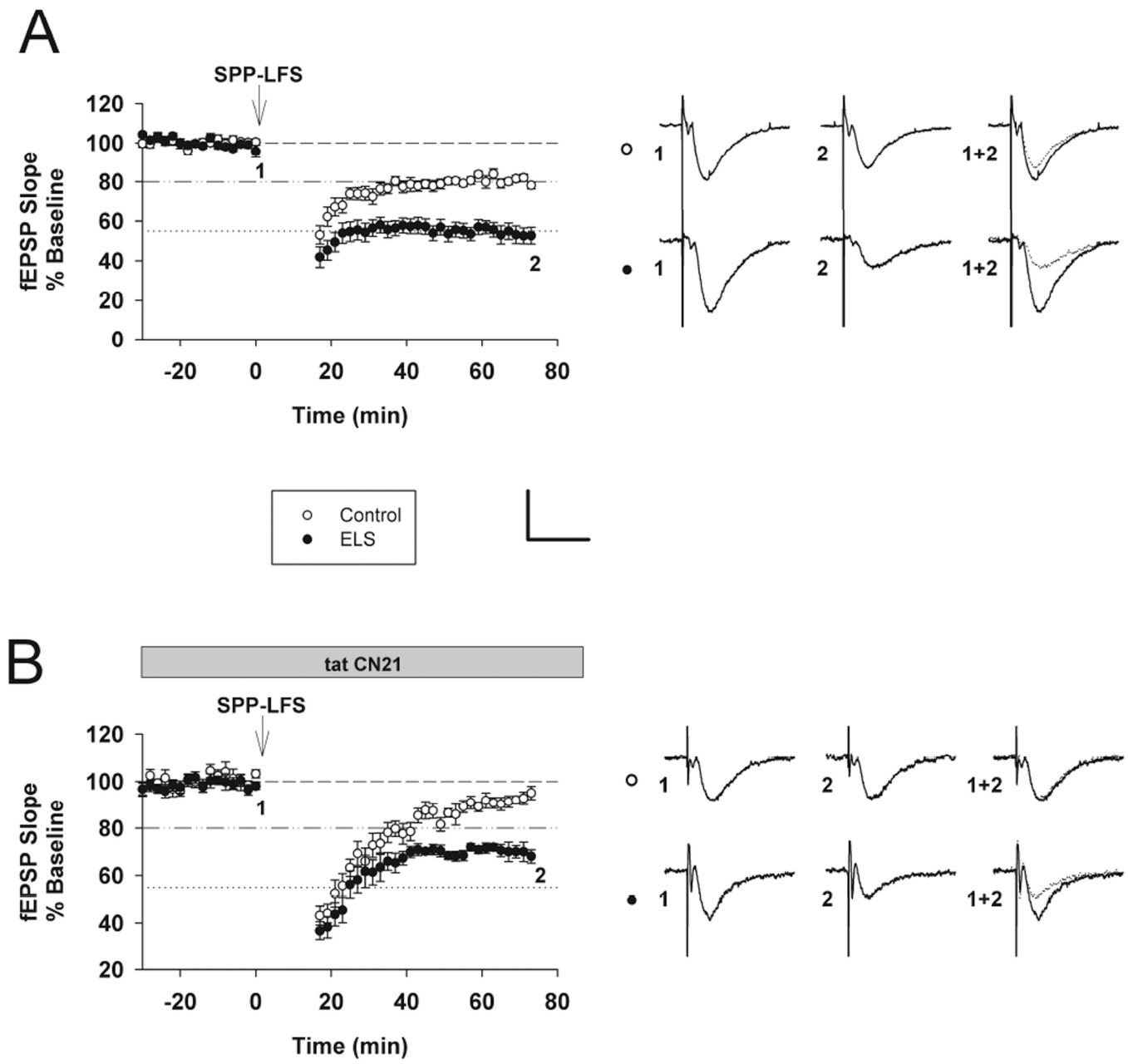

Figure 3. Enhanced mGluR-LTD following ELS in adult rats and the altered role of CaMKII in mGluR-LTD induction

A, Interleaved (vehicle, no inhibitor) mGluR-LTD experiments (control: 80.32 ± 1.56%, n = 18, ELS: 53.50 ± 3.99%, n = 18, P < 0.001, Student's t-test). B, Inhibition of CaMKII by tatCN21 (2 μM) completely blocked mGluR-LTD in control rats yet mGluR-LTD was still present in ELS rats (control: 93.72 ± 1.31%, n = 11, ELS: 68.39 ± 1.98%, n = 10, P < 0.001, Student's t-test). Insets show averages of 4 fEPSPs near the numerically indicated time points. Scale bar 0.5 mV × 15 ms. Dashed line indicates baseline; Dashed/dotted line indicates average control mGluR-LTD (vehicle, no inhibitors from (A)) used in subsequent Figures; Dotted line indicates average ELS mGluR-LTD (vehicle, no inhibitors from (A)) used in subsequent Figures.

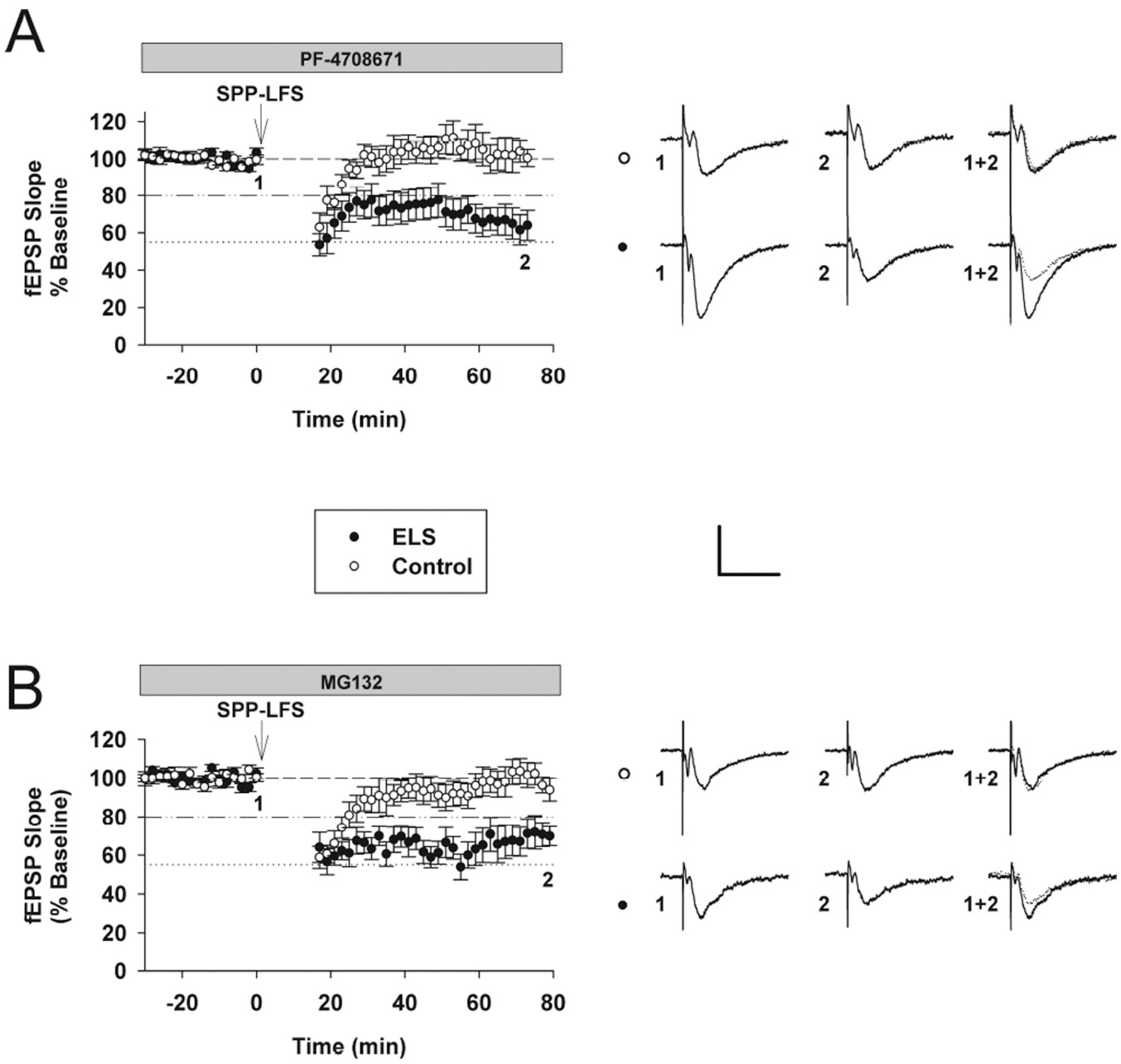

Figure 4. The role of S6K and the proteasome in mGluR-LTD induction was altered after ELS

A, The S6K inhibitor PF-4708671 (25 μM) completely blocked mGluR-LTD in controls, yet mGluR-LTD was still present in ELS rats (control: 106.14. ± 9.71%, n = 6, ELS: 54.96±8.75%, n = 10, P < 0.01, Student's t-test). B, The proteasomal inhibitor MG-132 (10 μM) completely blocked mGluR-LTD in controls, yet mGluR-LTD was still present in ELS rats (control: 99.93 ± 6.05%, n = 8, ELS: 62.93 ± 7.83%, n = 6, P = 0.0025, Student's t-test). Insets show averages of 4 fEPSPs near the numerically indicated time points. Scale bar 0.5 mV × 15 ms. Dashed line indicates baseline; dashed/dotted line indicates average control mGluR-LTD (vehicle, no inhibitors); dotted line indicates average ELS mGluR-LTD (vehicle, no inhibitors).

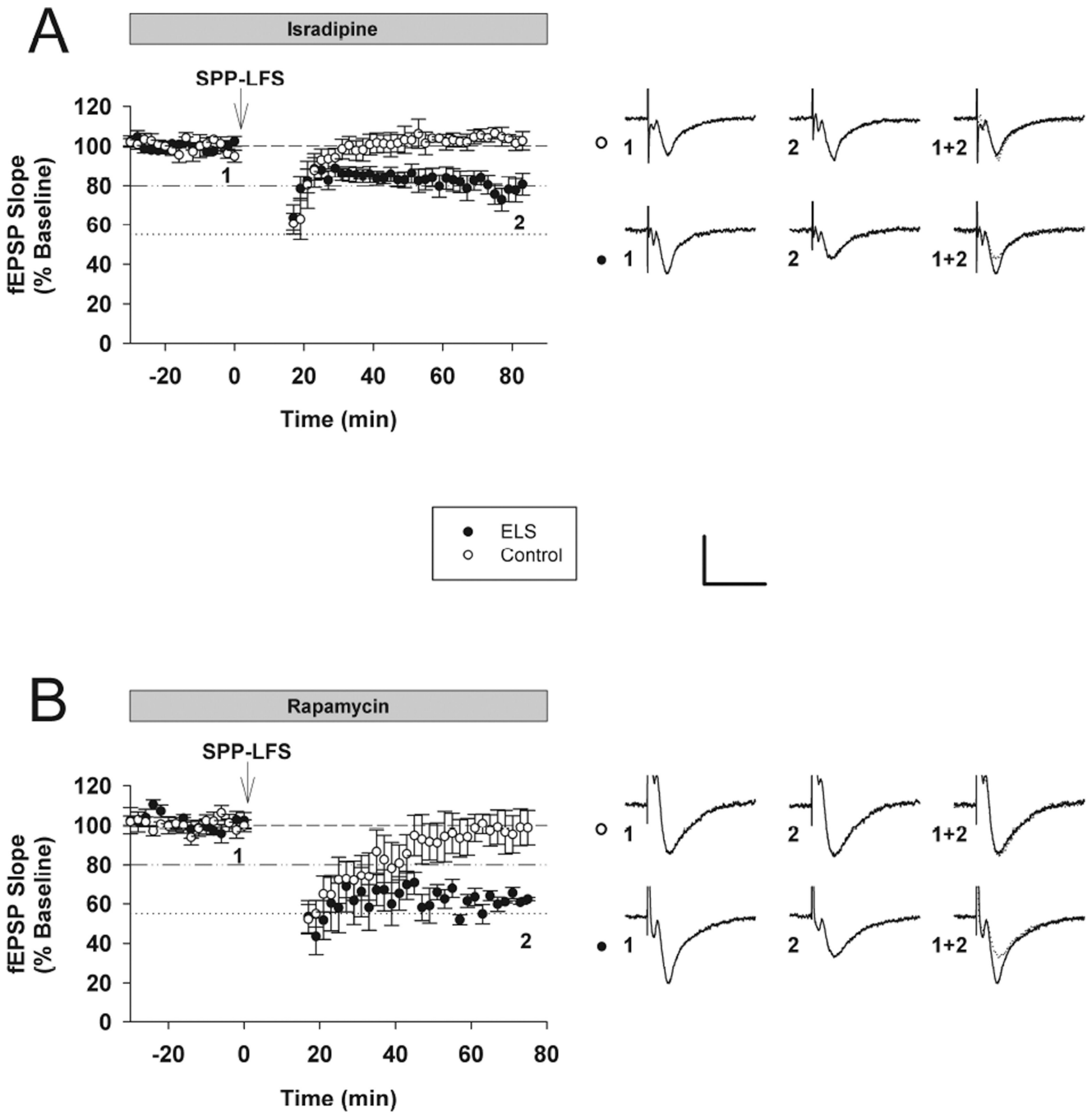

Figure 5. The role of L-type VGCCs and mTOR in mGluR-LTD induction was altered after ELS

A, mGluR-LTD was completely blocked in control rats in the presence of the L-type voltage-gated calcium channel antagonist isradipine (10 μm), yet mGluR-LTD was still present in ELS rats (control with isradipine: 100.44 ± 4.70%, n = 5, ELS with isradipine: 75.67 ± 5.26%, n = 9, $P < 0.01$, Student's t-test). B, mGluR-LTD was completely blocked in control rats in the presence of the mTOR antagonist rapamycin (20 nM), yet mGluR-LTD was still present in ELS rats(control: 96.71 ± 2.45%, n = 7, ELS: 58.09 ± 7.20%, n = 5, $P < 0.001$, Student's t-test). Insets show averages of 4 fEPSPs near the numerically indicated

time points. Scale bar 0.5 mV × 15 ms. Dashed line indicates baseline; dashed/dotted line indicates average control mGluR-LTD (vehicle, no inhibitors); dotted line indicates average ELS mGluR-LTD (vehicle, no inhibitors).

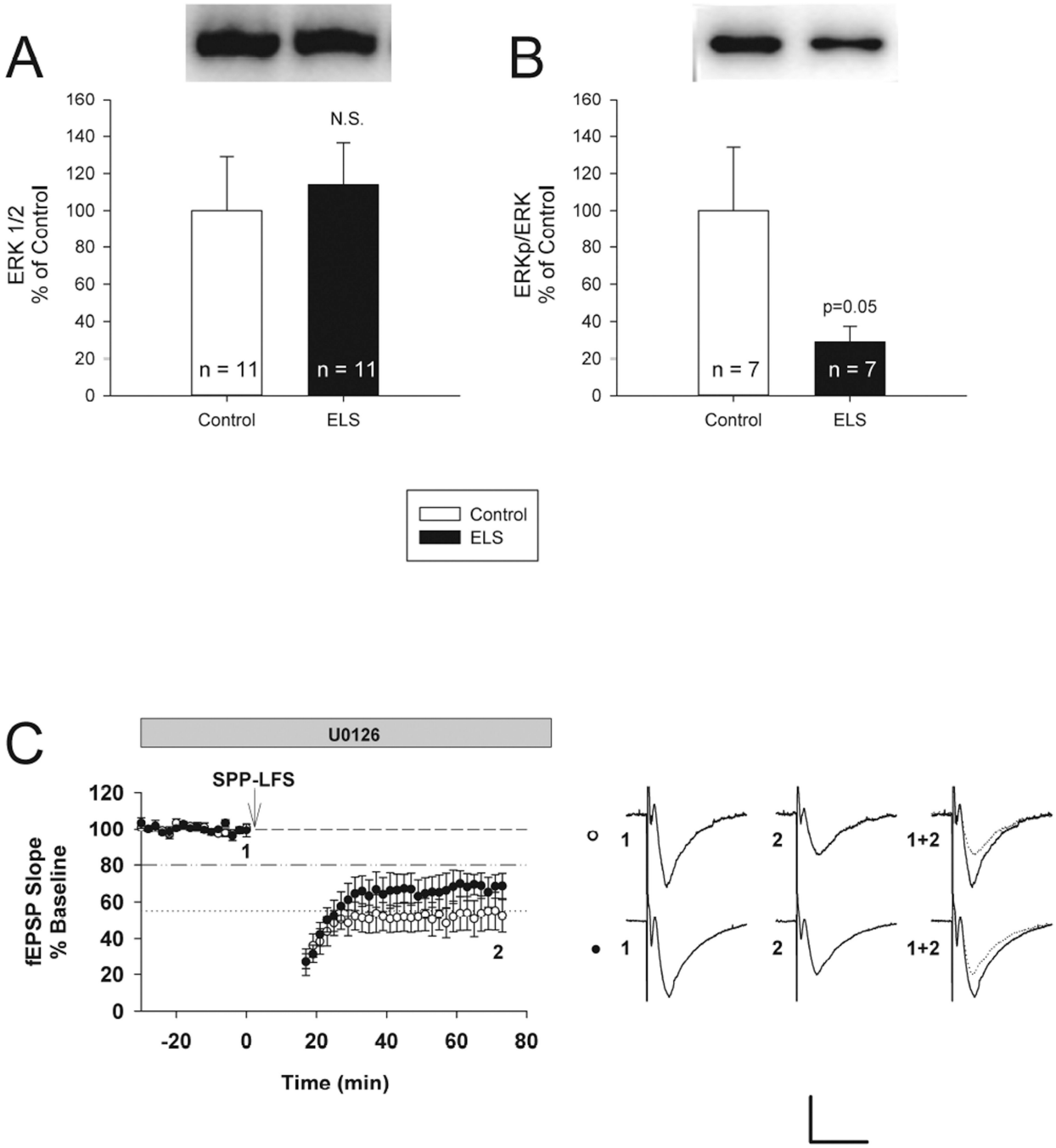

Figure 6. Reduced phosphorylation of ERK and role of ERK inhibition following ELS

A, ELS caused no changes in expression of total ERK (control: 100.00 ± 29.05%, n = 11, ELS: 113.97 ± 22.50%, n = 11, P = NS, Student's t-test). B, ELS caused significantly reduced phosphorylation of ERK at Thr202/Tyr204 (control: 100.00 ± 34.12%, n = 7, ELS: 28.88 ± 8.52%, n = 8, P < 0.05, Student's t-test). Semi-quantitative western-blot technique (Cornejo et al., 2007) was used to determine immunoreactivity/mg loaded protein, which were normalized to controls (see Methods). C, The MEK/ERK 1/2 inhibitor U0126 (5 μM) did not significantly alter mGluR-LTD between ELS and controls (control: 46.97 ± 9.56%, n

= 7, ELS: 68.77 ± 6.06%, n = 7, P < 0.08, Student's t-test). Scale bar 0.5 mV × 15 ms. Dashed line indicates baseline; dashed/dotted line indicates average control mGluR-LTD (vehicle, no inhibitors); dotted line indicates average ELS mGluR-LTD (vehicle, no inhibitors).

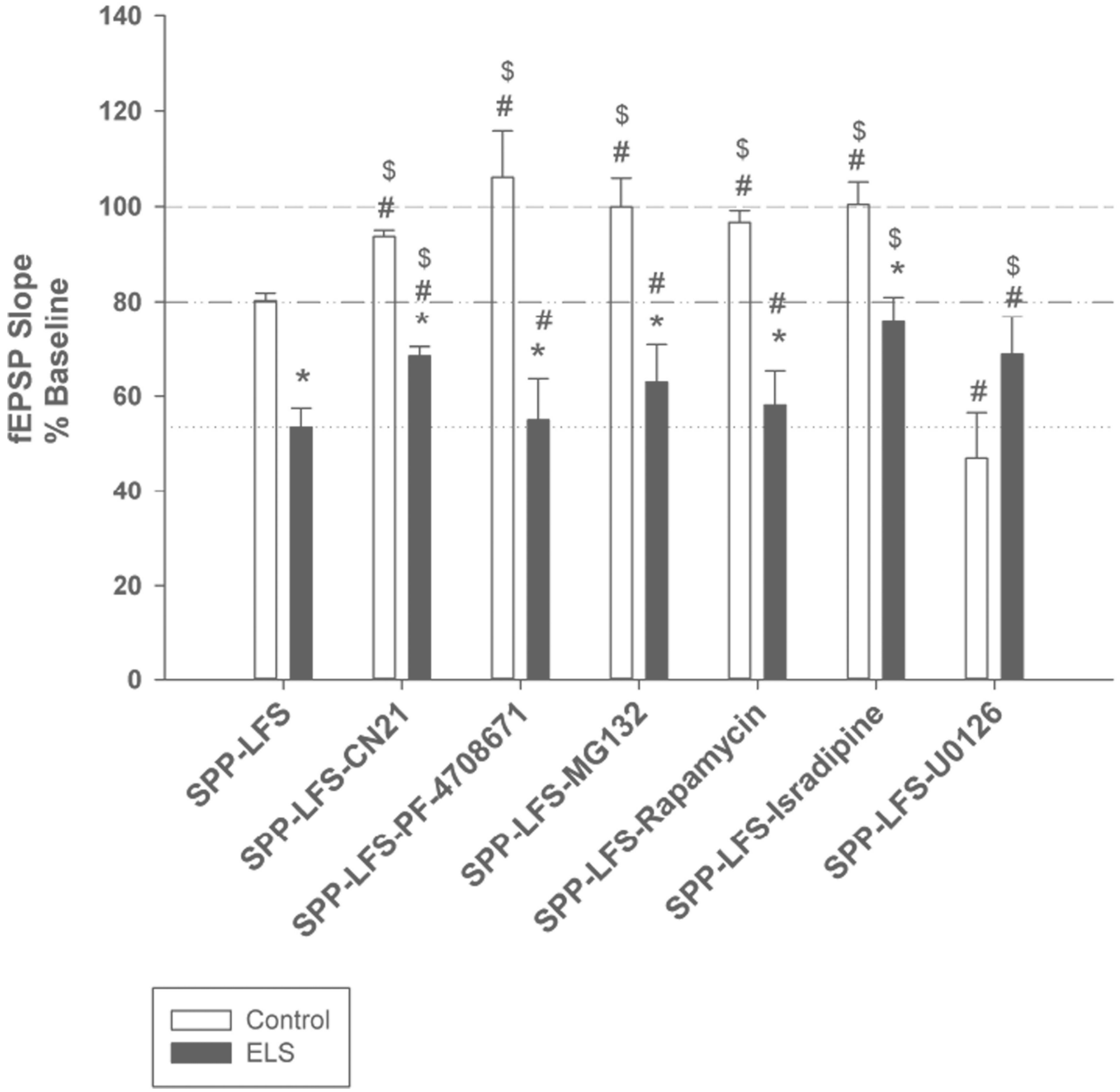

Figure 7. Summary of mGluR-LTD experiments

* - indicates significantly different than similarly treated control; # - indicates significantly different than naïve control mGluR-LTD (vehicle, no inhibitors); $ - indicates significantly different from naïve ELS mGluR-LTD (vehicle, no inhibitors). Dashed line indicates baseline; dashed/dotted line indicates average control mGluR-LTD (vehicle, no inhibitors); dotted line indicates average ELS mGluR-LTD (vehicle, no inhibitors).

Table 1

Primary antibodies used for western-blot analysis.

Primary Antibody	size kDa	dilutent	Host name	dilution factor	company
AKAP150	150	1%milk	rab	1//2000	Dell'Aquca lab
ARC	55	5%milk	mouse	1/500	BD Transduction Laboratories
CAMKII P T286	50/60	1%milk	rab	1//2000	Phosphosolutions
CAMKII P T305	50	1%BSA	rab	1//1000	Phosphosolutions
CAMKII	50/60	1%milk	mouse	1//3000	BD Transduction Laboratories
ERK1/2 P(Thr202/Tyr204)	42/44	5%milk	mouse	1//2000	Cell Signaling
ERK1/2	42/44	5%BSA	rab	1/1000	Cell Signaling
GLUR1	110	1%BSA	rab	1/1000	Millipore
GLUR1 P845	100	1%milk	rab	1/500	Phosphosolutions
GLUR1 P831	100	1%BSA	rab	1/500	Phosphosolutions
MECP2	75	1%milk	rab	1/1000	Millipore
MECP2 P	52	1%milk	rab	1/500	ABGENT
neuroligin 1(A-4)	101	1%milk	mouse	1/100	Santa Cruz Biologicals
neuroligin 3 (H-55)	88	1%milk	rab	1/200	Santa Cruz Biologicals
NSF	78	5%milk	rab	1/1000	Cell Signaling
P38 MAPK	40	1%milk	rab	1/500	Cell Signaling
P38 MAPK P (Thr180/Tyr182)	40	1%BSA	rab	1/500	Cell Signaling
PICK1	55	1%milk	rab	1/500	Millipore
SAP97	140	1%milk	rab	1/1000	Thermo Scientific
SAP102	102	1%milk	mouse	1/1000	UC Davis/NIH NeuroMab Facility
SNAP23	27	1%milk	rab	1/500	Abcam
SYP	38	1%milk	rab	1//2000	Santa Cruz Biologicals
VGAT	55	1%milk	rab	1/500	Millipore

Table 2

Comprehensive screening of mGluR-LTD related proteins following ELS in adult rats. Specific proteins were selected as targets of phosphatases or kinases that are altered in the ELS model (such as CaMKII) or because they are associated with the cellular mechanisms of synaptic plasticity. Semi-quantitative western-blot technique (Cornejo et al., 2007) was used to determine immunoreactivity/mg loaded protein, which were normalized to controls (see Methods).

Antibody	Mean ± S.E.M control	n value	Mean ± S.E.M ELS	n value	P value	Summary
AKAP150	100.00± 11.17	n=12	76.84±5.86	n=13	0.073	
ARC	100.00±7.31	n=10	86.13±11.50	n=10	0.385	
CAMKII β P T286/CAMKII β	100.00±27.50	n=9	1213.33±262.78	n=11	P<0.02	ELS higher
CAMKII α P T286/CAMK II α	100.00±27.74	n=9	660.84±182.85	n=8	P<0.001	ELS higher
CAMKII P T305/ CAMKII	100.00±18.89	n=12	95.13±25.22	n=13	0.575	
CAMKII β	100.00±9.06	n=9	106.60±16.10	n=12	0.644	
CAMKII ALPHA	100.00±15.90	n=12	84.90±13.80	n=11	0.485	
ERK1/2 P/ERK1/2	100.00±34.12	n=7	28.88±8.52	n=8	P<0.05	control higher
ERK1/2	100.00±29.05	n=11	113.97±22.50	n=11	0.707	
GLUR1	100.00±9.42	n=9	86.43±6.93	n=7	0.289	
GLUR1 P845/GLUR1	100.00±19.82	n=10	94.93±7.83	n=9	0.322	
GLUR1 P831/GLUR1	100.00±20.83	n=12	73.89±9.27	n=13	0.348	
MECP2	100.00±6.93	n=8	85.79±6.04	n=7	0.142	
MECP2 P/MECP2	100.00±12.10	n=8	132.27±23.14	n=11	0.338	
Neuroligin1	100.00±23.12	n=11	133.25±28.83	n=11	0.377	
Neuroligin3	100.00±4.47	n=9	86.94±3.55	n=11	P =0.032	control higher
NSF	100.00±14.40	n=13	116.84±14.40	n=6	0.423	
P38 MAPK	100.00±10.47	n=10	94.21±11.21	n=8	0.712	
P38 MAPK P/p38 MAPK	100.00±33.20	n=9	83.20±18.00	n=9	0.397	
PICK1	100.00±12.26	n=10	78.78±11.91	n=13	0.235	
SAP97	100.00±8.45	n=9	107.29±5.76	n=7	0.515	

Antibody	Mean ± S.E.M control	n value	Mean ± S.E.M ELS	n value	P value	Summary
SAP102	100.00±5.22	n=17	100.97±8.51	n=19	0.428	
SNAP23	100.00±14.05	n=10	92.04±15.05	n=11	0.477	
SYP	100.00±14.7	n=19	116.31±17.91	n=19	0.431	
VGAT	100.00±13.81	n=9	94.68±12.97	n=7	0.784	